

Article

Analysis and Estimation of Geographical and Topographic Influencing Factors for Precipitation Distribution over Complex Terrains: A Case of the Northeast Slope of the Qinghai–Tibet Plateau

Weicheng Liu ^{1,2}, Qiang Zhang ^{1,3,4,*}, Zhao Fu ^{2,*}, Xiaoyan Chen ² and Hong Li ²

¹ College of Atmospheric Sciences, Lanzhou University, Lanzhou 730000, China; cnliuwc@163.com

² Lanzhou Central Meteorological Observatory, Lanzhou 730020, China; chenchensjh@163.com (X.C.); lih2010@lzu.edu.cn (H.L.)

³ Key Laboratory of Arid Climatic Change and Disaster Reduction of Gansu Province/China Meteorological Administrator, Lanzhou 730020, China

⁴ Institute of Arid Meteorology, China Meteorological Administrator, Lanzhou 730020, China

* Correspondence: zhangqiang@cma.gov.cn (Q.Z.); dry52889@163.com (Z.F.)

Received: 31 May 2018; Accepted: 8 August 2018; Published: 7 September 2018



Abstract: Due to the complex terrain, sparse precipitation observation sites, and uneven distribution of precipitation in the northeastern slope of the Qinghai–Tibet Plateau, it is necessary to establish a precipitation estimation method with strong applicability. In this study, the precipitation observation data from meteorological stations in the northeast slope of the Qinghai–Tibet Plateau and 11 geographical and topographic factors related to precipitation distribution were used to analyze the main factors affecting precipitation distribution. Based on the above, a multivariate linear regression precipitation estimation model was established. The results revealed that precipitation is negatively related to latitude and elevation, but positively related to longitude and slope for stations with an elevation below 1700 m. Meanwhile, precipitation shows positive correlations with both latitude and longitude, and negative correlations with elevation for stations with elevations above 1700 m. The established multivariate regression precipitation estimating model performs better at estimating the mean annual precipitation in autumn, summer, and spring, and is less accurate in winter. In contrast, the multivariate regression mode combined with the residual error correction method can effectively improve the precipitation forecast ability. The model is applicable to the unique natural geographical features of the northeast slope of the Qinghai–Tibet Plateau. The research results are of great significance for analyzing the temporal and spatial distribution pattern of precipitation in complex terrain areas.

Keywords: complex terrains; geographical and topographical factors; precipitation estimation; Northeast Slope of Qinghai–Tibet Plateau; multivariate regression; residual error correction

1. Introduction

Information about the spatial distribution of precipitation is vital for the research and applications of fields such as meteorology, hydrology, agriculture, ecology, and environmental science [1–3]. In normal cases, the precipitation distribution is mainly determined by the large-scale atmospheric circulation; however, for regions with complex terrain, the terrain can render precipitation distribution rules by affecting the large-scale weather system, atmospheric airflow, and microphysical processes of clouds [4–6]. In the meantime, geographical factors can also influence the precipitation distribution through solar radiation [7], melting-layer height [8], and vapor source distance [9], which differ a lot in different locations.

Nevertheless, in situ precipitation observations are sparse in space in recent years. In addition, newly supplemented stations have short data series, so they fail to provide favorable information for depicting the spatial change patterns of precipitation. Alternatively, spatial interpolation technology can predict the values beyond observation coverage based on observed values. Therefore, interpolation technology based on geographical and topographical impact factors has the potential of turning into an important means of precipitation distribution estimation. In recent years, many experts and scholars have set out to study the impact of geographical and topographical factors on the precipitation distribution in different regions or areas, and established a variety of precipitation distribution estimating methods. Briefly, the geographical and topographical factors that influence the precipitation distribution in different areas, including the longitude, latitude [10], station elevation [9], maximum height of mountains facing different directions [11], average elevation of the station's vicinity [12], slope, exposure, average slope and exposure in the vicinity of the station, distance from vapor source, distance from ridge [10], and landform type [13]. The precipitation estimating modes that have been established based on the aforesaid factors cover artificial neural network (ANN) [10], partial least squares regression (PLS) [14], and MLR (multivariate linear regression) [14], in which MLR remains relatively simple and takes into consideration the overlapping effect of different factors in order to reduce its estimation error [15].

The northeast slope of the Qinghai–Tibet Plateau is located at the junction between the east section of Qilian Mountain and the Qinling mountains. It is in a marginal area of westerly climate, plateau climate, and southeast Asian monsoon climate, as well as the transitional belt between the southeastern moist monsoon climate and the northwestern inland arid climate. Affected by the complex plateau terrain, a sub-synoptic scale system is formed with the mean circulation within the boundary layer of the northeast slope of the Qinghai–Tibet Plateau. Such a sub-synoptic scale circulation system can lead to extremely uneven thermal or dynamic effect in the local area, so that the spatial distribution of precipitation in the area becomes much non-uniform, and environmental issues such as water and soil loss, grassland deterioration, and desertization are quite prominent [16]. According to the study of Zhang et al. [17], in the east of the Qinghai–Tibet Plateau, the precipitation displayed a significant decrease when the elevation was 340–1400 m; it then gradually increase with rising elevation. When the elevation reached 3600 m, the precipitation fell again with the increase of elevation. Wei et al. [18] used eight interpolation methods and a combined method of multivariate weighted regression and residual distribution to estimate the average annual precipitation distribution in Dingxi, the area of the northeast slope of the Tibetan plateau. The results showed that the accuracy of the combined method is the best. Peng et al. [19] investigated the precipitation distribution in the Qilian mountains, and found that the topography and wind direction are the main factors that affect the precipitation distribution in this area. Also, the mountain microclimate simulation model (MTCLIM) was improved, and an algorithm suitable for estimating the daily precipitation in the mountain area was established. Yu et al. [20] used different spatial interpolation methods (ordinary Kriging, inverse distance weighting, and the radial basis function method) to estimate the annual precipitation in the Loess Plateau. The results showed that the ordinary Kriging interpolation method that employed the semivariogram as the ring model performed better, and the minimum average absolute error was 32.34 mm.

The previous studies have analyzed the advantages and disadvantages of different interpolation and estimation methods for precipitation estimation in the northeastern slope region of the Tibetan Plateau. However, few studies have focused on how geographic and topographic factors affect the precipitation distribution in this region. Also, the establishment of more accurate precipitation estimation algorithms based on the main influencing factors are still needed. Therefore, a better understanding of how the geographical and topographical factors affect the precipitation distribution in the complex terrains of the northeast Slope of the Qinghai–Tibet Plateau and their mechanisms and conduct subsequent precipitation distribution estimation are of great guiding significance for the analysis of local water resources distribution and climatic background for early warning of drought and flooding. In consideration of the complex terrains in the northeast slope of the Qinghai–Tibet Plateau,

the paper makes use of the digital elevation model (DEM) to find out different geographical and topographical factors and figure out the correlation coefficients of those factors with the precipitation. Based on the above, this work endeavors to build a model that is suitable to estimate the annual and quarterly average precipitation distribution in such an area.

2. Study Area

The northeast slope of the Qinghai–Tibet Plateau is situated at 101~109° E and 32~38° N in the junction of the Qinghai–Tibet Plateau, Loess Plateau, and Inner Mongolian Plateau. Its west constitutes the main body of the Qinghai–Tibet Plateau, its east belongs to the Loess Plateau, and the middle is a transitional area between the two terrains (Figure 1). In this area, the terrains are complicated, and the elevation varies from between 236–5388 m. Besides the Qinghai–Tibet Plateau, there are mountains such as Qilian Mountain, Liupan Mountain, and the Qingling mountains. The area is distributed with all sorts of landforms, including plateaus, hilly land, desert, Gobi, and plain. The northeast slope of the Qinghai–Tibet Plateau is far inland, and is far away from the sea. Moist airflow is obstructed here by such high terrains, which causes there to be little rainfall in the west regions, and further results in a dry climate and fragile ecology. Rather, the east is within the marginal area of the monsoon system, so the annual precipitation there is abundant, and regional annual average precipitation reaches 171.1–1275.7 mm.

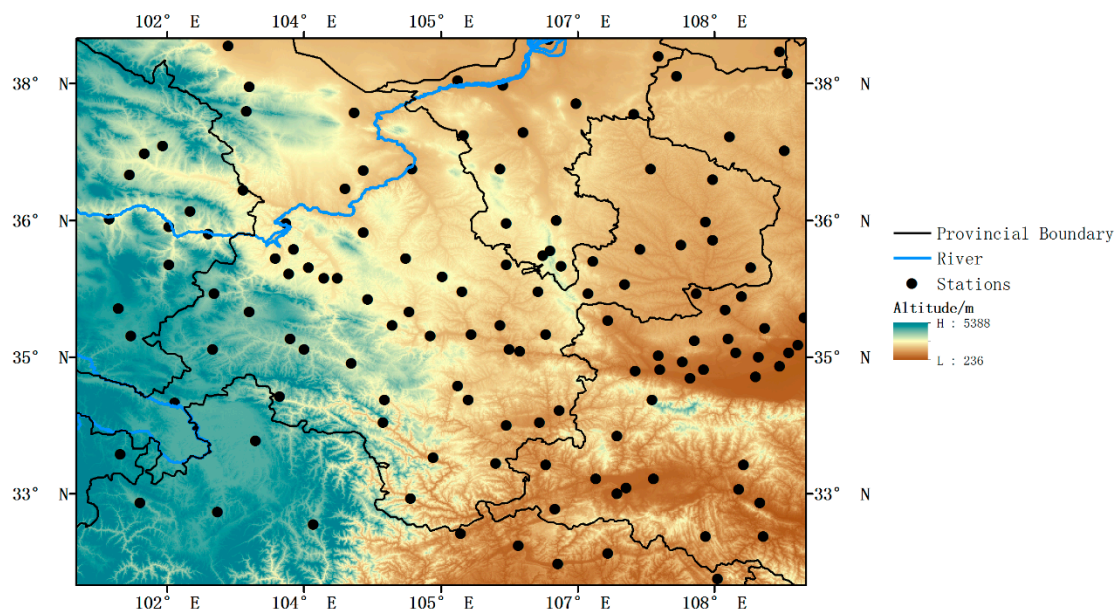


Figure 1. Study area.

3. Materials and Methods

3.1. Datasets

Monthly precipitation observing data of the northeast slope of the Qinghai–Tibet Plateau was collected from the standard monthly datasets of Chinese surface climate [21]. To test the reliability and continuity of the observed data, data from all of the stations underwent preliminary screening. Only stations with years of correct observation records exceeding 80% of all of the years, and no more than three consecutive years lacking relevant records were employed. Finally, 130 observation stations were chosen (Figure 1). Since the datasets already received strict quality control procedures such as extreme value checks and temporal/spatial consistency checks [22], only some missing values were interpolated in the data analysis. This means that when a specific station had observation values missed, the distance weight algorithm was used to interpolate the observations of the nearest site, which was

well-correlated ($r^2 > 0.95$) to the site with missing values [23]. The seasonal data were accumulated with monthly ones. Four seasons were divided by a meteorological perspective: spring (March–May), summer (June–August), autumn (September–November), and winter (December–February of following year).

DEM data were from global elevation data with a resolution of 90 m from the Shuttle Radar Topography Mission (SRTM) led by the American National Aeronautics and Space Administration (NASA) [24]. Topographical and geographical factors for all of the stations were derived from the DEM data using ArcGIS (ESRI, Redlands, CA, USA) and off-the-shelf ArcGIS software packages (Table 1). According to the study of Al-Ahmadi et al. [9], computation error increased as the factor resolution increased. Thus, in the present paper, different resolutions were adopted for a further study.

Table 1. Geographical and topographical factors.

Parameters	Units	Resolution
Latitude (Lat)	Degrees	0.001°
Longitude (Lon)	Degrees	0.001°
Altitude (Alt)	Meters	250 m
Mean altitude within a 5-km radius (Malt)	Meters	250 m
Mean slope within a 5-km radius (Ms)	Degrees	1°
Mean aspect within a 10-km radius (Masp)	Degrees	1°
Tangent of the average aspect within a 10-km radius (Tm)	-	0.01
Maximum altitude of the eastern sector within a 50-km radius (MaE)	Meters	250 m
Maximum altitude of the southern sector within a 50-km radius (MaS)	Meters	250 m
Maximum altitude of the western sector within a 50-km radius (MaW)	Meters	250 m
Maximum altitude of the northern sector within a 50-km radius (MaN)	Meters	250 m

3.2. Methods

The Pearson coefficient of correlation was utilized to figure out the correlation between precipitation distribution and geographical and topographical factors in the northeast slope of the Qinghai–Tibet Plateau [25,26]. Through an analysis of higher correlation coefficients, the factors affecting the precipitation distribution in the local area were determined. The detailed formulation was as follows:

$$R = \frac{n\sum \beta_i o_i - \sum \beta_i \sum o_i}{\sqrt{[n\sum \beta_i^2 - (\sum \beta_i)^2][n\sum o_i^2 - (\sum o_i)^2]}} \tag{1}$$

where R is the correlation coefficient, o_i is the observed precipitation value, β_i is the geographical or topographical factor, and n is the number of samples involved in the calculation.

A precipitation distribution estimation model about the research area was built through multivariable stepwise linear regression (MSLR) on the basis of geographical and topographical factors [27]. Stepwise regression is a method of fitting regression models. In each step, a variable is considered for addition to or subtraction from the set of explanatory variables based on some prespecified criterion. The adjusted \bar{R}^2 resulting from each calculation was tested to reserve only the independent variables with significant effect until no variable could be added or subtracted. At this time, the regression equation was considered as the optimal estimating model. The paper chose a forward selection strategy, which meant that the model started from no variable at all, and then a geographical/topographical factor with most significant fitting effect was added step by step until no factor should be added.

The linear regression estimating model is:

$$y_i = \beta_0 + \beta_1 x_{1i} + \beta_2 x_{2i} + \dots + \beta_n x_{ni} \tag{2}$$

where y means the estimated precipitation, x_n ($n = 1, 2, \dots$) means the geographical/topographical factor, β_0 means the intercept of the regression equation, β_n ($n = 1, 2, \dots$) means the regression coefficient, and i means the regression computation sample. The computation formula about adjusted \bar{R}^2 is as follows:

$$\bar{R}^2 = 1 - (1 - R^2) \frac{n-1}{n-p} \quad (3)$$

where p indicates the number of geographical/topographical factors in the regression model, n is the number of regression computation samples, and R^2 is the coefficient of multivariate regression determination, which decides the goodness-of-fit of the regression equation, and can be expressed as:

$$R^2 = \frac{\sum (p_i - \bar{o})^2}{\sum (o_i - \bar{o})^2} \quad (4)$$

where o_i and p_i are the observed precipitation and regression-estimated precipitation, respectively, and \bar{o} is the average observed precipitation.

The cross-validation method is a statistical analysis method that is used to verify the performance of the classifier [28]. It can be used to test the accuracy of the algorithm and obtain the optimal mathematical model. In this paper, the K-fold cross-validation method [29] is adopted; that is, the calculation site set is randomly divided into K subsets, and each subset data is separately verified as a model verification set, and the remaining K-1 subsets data is used as a model establishment set, so that K models will be obtained. Then, the verification subset is utilized to calculate the root mean square error (RMSE) of each model; the one with the smallest RMSE in the K models is selected as the optimal precipitation estimation model.

The estimation error of each station was computed after the precipitation distribution estimating model was established on the basis of the modeling subset, and “estimating error distribution” was derived from the errors of all of the stations. Afterwards, three algorithms—namely inverse distance weighted (IDW) [30–32], local polynomial interpolation (LPI) [33], and ordinary Kriging (OK) [34,35]—were adopted to interpolate the estimating errors into the whole computational domain, whereas the model verification subset got to acquire different estimating errors of all of the stations according to the interpolated error distribution.

The verification of precipitation estimation was done by comparing the observed values from stations in the model verification subset with the model estimating values. In the estimating effect check, four statistical estimation indicators were used [36]: the Pearson coefficient of correlation (R), mean error (ME), mean absolute error (MAE), and root mean square error ($RMSE$), whose detailed definitions are listed below:

$$ME = \frac{1}{n} \sum (p_i - o_i) / o_i \quad (5)$$

$$MAE = \frac{1}{n} \sum |p_i - o_i| / o_i \quad (6)$$

$$RMSE = \sqrt{\frac{\sum (p_i - o_i)^2}{n}} \quad (7)$$

where o_i and p_i are the observed precipitation and regression-estimated precipitation, and n is the number of verification samples. In order to effectively describe the seasonable change feature of precipitation distribution, all of the statistical indicators were presented with a percentage in relation to observed precipitation.

4. Results

4.1. Precipitation Affecting Factors

An analysis of the Pearson coefficient of correlation between annual and quarterly average precipitation and geographical/topographical factors on the northeast slope of the Qinghai–Tibet Plateau reveals (Table 2) a significant negative correlation between precipitation and latitude. It indicates declining precipitation with more northward stations, with the highest correlation coefficient among all of the factors. However, a consistent positive correlation is found between precipitation and longitude, which means the precipitation rises gradually from west to east on the northeastern slope of the Plateau. Precipitation was negatively related to the average station elevation, and the average elevation of the station vicinity with a 5-km radius, but the positive correlation with the latter tended to be more significant. It was also significantly and positively related to the average slope of the station vicinity with a 10-km radius, which suggested that the steeper the terrain, the higher the precipitation; it was consistently and positive related to the average exposure of the station vicinity with a 10-km radius, in spite of a much lower correlation. As to the highest elevations with different exposures, their correlations with precipitation differed materially, and only the winter precipitation presented a high negative correlation with the highest elevation on four exposures.

Table 2. Correlation coefficients between the total seasonal and annual precipitation and the geographical and topographical factors (all stations).

Parameters	Spring	Summer	Autumn	Winter	Annual
Lat	−0.88 **	−0.79 **	−0.86 **	−0.72 **	−0.84 **
Lon	0.17	0.24 **	0.37 **	0.45 **	0.28 **
Alt	−0.19 *	−0.24 *	−0.38 **	−0.38 **	−0.28 **
Malt	−0.06	−0.12	−0.22 *	−0.31 **	−0.15
Ms	0.37 **	0.31 **	0.32 **	0.28 **	0.33 **
Tm	0.19	0.18	0.17	0.16	0.18
MaE	0.11	0.01	−0.09	−0.25 **	−0.01
MaS	0.06	−0.04	−0.14	−0.26 **	−0.06
MaW	0.16	0.10	−0.02	−0.16	0.07
MaN	0.12	0.05	−0.06	−0.21 *	0.02

* Denote statistically significant at the 10% significance level. ** Denote statistically significant at the 5% significance level.

In order to find out the relationship between precipitation and elevation, the mean annual precipitation at stations with different elevations on the northeast slope of Qinghai–Tibet Plateau was analyzed, and it was obvious that the precipitation distribution differed greatly under different elevations (Figure 2). The precipitation is highly negatively correlated to elevation. This was in agreement with the previous correlation, which analyzed the outcome. Further analysis suggested an evident sudden “inflection point” of precipitation with the change of elevation. On both sides of that inflection point, the precipitation changed with the elevation in two distinct ways. The inflection point was situated at an elevation of about 1400–1900 m. The precipitation at stations with an elevation higher than 1900 m is positively correlated to the elevation, while it was negatively correlated to the elevation for stations below 1400 m. To determine the position of the inflection point accurately, six thresholds were chosen between 1400–1900 m, with 100-m intervals. All of the stations were divided into two intervals as per each threshold (namely, the stations no lower than the threshold, and those above it), in order to figure out the correlation between the precipitation of stations in two intervals and the elevation for each threshold. It was found that when the threshold was 1700 m, the correlation of both intervals became quite significant. Therefore, 1700 m was determined to be the inflection point.

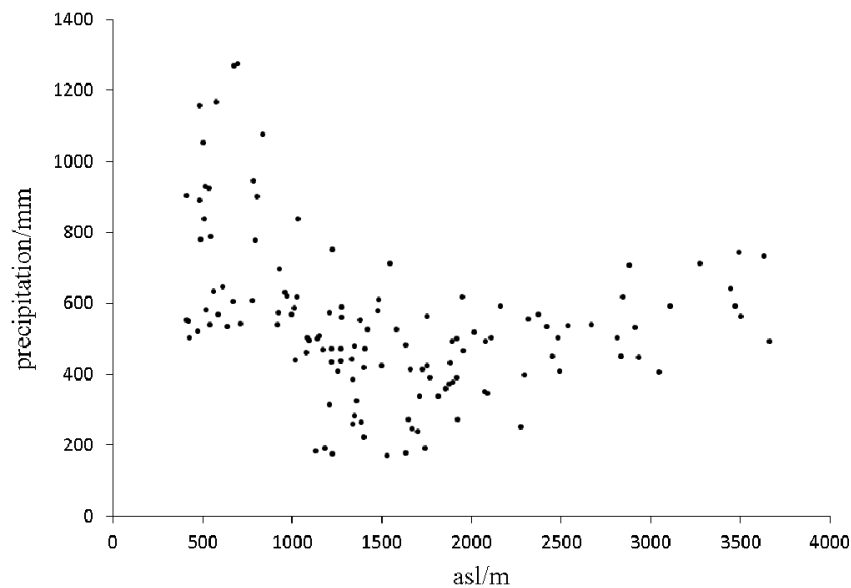


Figure 2. Precipitation distribution at different elevations.

For the stations with elevations below 1700 m (Table 3), which included 82 stations, the annual and quarterly mean precipitation appeared to be significantly and negatively related to the latitude, which could be attributed to the melting-layer changes with the latitude. Existing studies have proved that the melting layer is lowered down against the rising latitude [37,38], and a higher melting layer is unfavorable for the generation of precipitation [39]. The positive correlation between precipitation and latitude became even more eye-catching in autumn and winter, because the stations with elevations below 1700 m are mainly distributed in the east of Gansu, the middle-south of Shaanxi, and north of Sichuan, where precipitation distribution was affected by the East Asian monsoon [23]. In such areas, the greater the stations' latitude, the closer the stations are to the vapor source, and the more easily the precipitation is generated. The annual and quarterly mean precipitation were negatively related to both station elevation and the average elevation of the station's vicinity, and the former's correlation was more significant. By contrast, the precipitation was proven to be significantly positively correlated to the average slope of the station's vicinity. This meant that a steeper terrain would facilitate the generation of precipitation. The reason why two factors exerted different effects on the precipitation was probably because the maximum water vapor content in the areas with an elevation below 1700 m on the northeast slope of the Qinghai–Tibet Plateau was in the lower layer of the atmosphere (850–700 hPa) [40]. The correlation between precipitation and the average exposure of the station's vicinity remained insignificant. When it came to the effect of maximum elevation in different directions on the precipitation, it seemed that only the maximum elevation in the west had a significant correlation with the precipitation in spring, summer, and autumn, which may be related to the region's water vapor being mainly derived from the East Asian monsoon [41]. When the East Asian monsoon carries a large amount of water vapor to the west, it is easy for the western mountains to converge and uplift to form precipitation.

Table 3. Same as Table 2, but for stations with an elevation below 1700 m.

Parameters	Spring	Summer	Autumn	Winter	Annual
Lat	−0.89 **	−0.81 **	−0.87 **	−0.74 **	−0.85 **
Lon	0.30 *	0.28 *	0.38 **	0.43 **	0.32 **
Alt	−0.65 **	−0.56 **	−0.70 **	−0.65 **	−0.63 **
Malt	−0.22	−0.23	−0.31 *	−0.36 **	−0.26 *
Ms	0.50 **	0.47 **	0.53 **	0.59 **	0.51 **
Tm	0.18	0.15	0.18	0.18	0.17
MaE	0.20	0.16	0.10	−0.10	0.14
MaS	0.07	0.02	−0.03	−0.16	0.01
MaW	0.34 **	0.33 **	0.25 *	0.08	0.30 *
MaN	0.21	0.21	0.14	−0.04	0.19

* Denote statistically significant at the 10% significance level. ** Denote statistically significant at the 5% significance level.

For the stations with elevations above 1700 m (Table 4), which included 48 stations, a consistent and highly significant negative correlation was found again between the annual and quarterly mean precipitation and the latitude. The correlation between precipitation and longitude displayed great discrepancy; the annual mean precipitation and precipitation in spring, summer, and autumn were negatively related to the longitude, whereas the precipitation in winter was positively related to it, regardless of the insignificant correlation. This was much unlike the stations below 1700 m, and it is mainly because most of the stations higher than 1700 m are distributed in the edge of the Qinghai–Tibet Plateau, the middle of Gansu, and south of Ningxia, where the westerlies’ activities exerted a dominating effect on local precipitation [23], and water vapor was delivered here along northwest and west paths [41]. The annual and quarterly mean precipitation were significantly and positively related to the station elevation and average elevation of the station’s vicinity, and correlation with the former was more significant. This was also obviously different from the stations with an elevation higher than 1700 m, and it may be in part explained by the maximum water vapor content being in the middle and upper layer (700~500 hPa) of the atmosphere [40]. The annual and quarterly mean precipitation were less correlated to the average slope of the station’s vicinity, and a great difference was spotted in their correlation with the average exposure. The mean precipitation kept being in positive correlation with the exposure in all of the seasons except for autumn, which indicated that the more westward and northward the average exposure of the station’s vicinity was, the more precipitation could be expected. As for the effect of the highest elevation in different directions on the precipitation, it was obvious that annual precipitation and precipitation in spring, summer, and autumn were positively related to the highest elevation in four directions. The effect of those factors on the precipitation may also be related to the sources of local water vapor.

Table 4. Same as Table 2, but for stations with an elevation above 1700 m.

Parameters	Spring	Summer	Autumn	Winter	Annual
Lat	−0.84 **	−0.71 **	−0.87 **	−0.65 **	−0.82 **
Lon	−0.24	−0.21	−0.22	0.18	−0.21
Alt	0.52 **	0.72 **	0.68 **	0.47 **	0.68 **
Malt	0.34 *	0.44 **	−0.44 **	0.11	0.42 **
Ms	0.22	0.10	−0.13	−0.12	0.14
Tm	0.28	0.42 *	−0.31	0.26	0.37 *
MaE	0.31	0.25	0.33 *	−0.05	0.28
MaS	0.39 *	0.35 *	0.40 *	0.03	0.38 *
MaW	0.26	0.30	0.33 *	−0.03	0.30
MaN	0.31	0.27	0.32	−0.04	0.30

* Denote statistically significant at the 10% significance level. ** Denote statistically significant at the 5% significance level.

4.2. Precipitation Estimating Model

Multivariate stepwise linear regression method and 10-fold cross-validation (the calculating stations are randomly divided into 10 subsets) were employed to build a best annual and quarterly mean precipitation estimating models (EM). The geographical and topographical factors used in the EMs are shown in Table 5. It could be found that the influencing factors used in different EMs differ a lot. All of the models covered three common factors, i.e., latitude (Lat), longitude (Lon), and elevation (Alt). The mean altitude around the station (Malt), the max elevation to the east of the station (MaE), and max elevation to the north of the station (MaN) are the second most used factors, and are used in two seasonal and annual average precipitation estimation models, respectively. The mean slope (Ms) around the station, the mean aspect of the station’s vicinity (Tm), and the maximum elevation to the south of the station (MaS) are only used in one seasonal precipitation estimation model. The winter precipitation estimation model uses the least parameters (only five of them), while the other models use seven parameters, but the different models use different parameters. By checking the adjusted \bar{R}^2 of different models, it was found that the mean precipitation estimating models for autumn and spring did best, followed by the annual mean precipitation estimating model. By contrast, the winter and summer precipitation estimating models failed to generate good performance. This may be due to the general low precipitation in winter and the greatly changing precipitation distribution in summer.

Table 5. Correlation coefficients between precipitation from different time scales and influence factors of the multivariate regression models.

Parameter	Spring	Summer	Autumn	Winter	Annual
(a) Coefficients β_n					
Lat	−23.697	−54.290	−32.320	−3.822	−115.069
Lon	7.230	23.157	15.087	1.762	50.916
Alt	0.013	0.038	0.012	0.002	0.065
Malt	−0.031	−0.094	−0.042		−0.176
Ms			0.983		
Tm	0.613				
MaE	0.010		0.010	0.003	0.026
MaS		−0.001			
MaW	0.018	0.065	0.029		0.107
MaN		0.018		−0.005	0.032
(b) Intercept β_0					
	142.634	−344.938	−371.816	−40.669	−982.122
(c) Adjusted coefficient of determination \bar{R}^2					
	0.81	0.70	0.84	0.71	0.79

Due to the factors influencing precipitation distribution being discrepant at different altitudes, the optimal precipitation estimation models are established for stations with altitudes of less than 1700 m and above 1700 m, respectively. The 10-fold cross-validation and the eight-fold cross-validation were used by the precipitation estimation model. The geographical and topographical factors used in the station precipitation estimating models by elevation were more different (Table 6). The precipitation estimating models for stations with an elevation below 1700 m (EMB)—Lat, Lon, Alt and Malt—were adopted, without Ms. Seven parameters were used in the spring, autumn, and annual average precipitation estimation models, while only six parameters were used in the summer and winter average precipitation estimation models. For the adjusted \bar{R}^2 , similar to MR, the precipitation estimating effect of the spring, autumn, and annual was better than that of summer and winter estimation. The adjusted \bar{R}^2 values of the spring and autumn precipitation estimation models were superior to that of the EM estimation model. As for the precipitation estimating models (EMA) of

stations higher than 1700 m, Lat and Alt were adopted to all of the models but without Ms, Tm, MaS, and MaW. Unlike EM and EMB, MaE was the second most used parameter in two seasonal and annual precipitation estimation models. Lon, Malt, and MaN are only used in one season’s estimation model. The winter precipitation estimation model used four parameters, while the remaining models contained three parameters. From the perspective of adjusted \bar{R}^2 values, the annual precipitation was best estimated, followed by autumn, summer, and winter in turn. Nevertheless, the overall estimating effect of EMA was obviously inferior to that of EM and EMB. This may be related to the non-uniform precipitation distribution of stations with an elevation higher than 1700 m.

Table 6. Same as Table 5, but for areas with an elevation below 1700 m (EMB) and above 1700 m (EMA), respectively.

Parameters	Spring	Summer	Autumn	Winter	Annual	Parameters	Spring	Summer	Autumn	Winter	Annual
	(EMB)						(EMA)				
	(a) Coefficients β_n						(a) Coefficients β_n				
Lat	−24.655	−60.277	−35.136	−3.487	−123.561	Lat	−19.322	−24.849	−18.74	−1.497	−63.504
Lon	11.059	25.36	15.931	1.57	53.599	Lon				1.464	
Alt	0.020	0.083	0.018	0.003	0.110	Alt	0.012	0.063	0.025	0.006	0.099
Malt	−0.04	−0.164	−0.069	−0.007	−0.237	Malt	−0.007				
Ms						Ms					
Tm				0.343		Tm					
MaE	0.022		0.010		0.108	MaE	−0.024	−0.010		−0.037	−0.024
MaS	−0.010				−0.082	MaS					
MaW	0.022	0.066	0.015	0.002	0.139	MaW					
MaN		0.056	0.023			MaN			−0.002		
	(b) Intercept β_0						(b) Intercept β_0				
	−241.158	−394.242	−337.254	−30.707	−939.533		771.326	1066.042	747.08		−95.496
	(c) Adjusted Coefficient of Determination \bar{R}^2						(c) Adjusted Coefficient of Determination \bar{R}^2				
	0.90	0.76	0.89	0.72	0.85		0.73	0.76	0.79	0.75	0.81

4.3. Precipitation Estimation Verification

For the precipitation estimating models established, the residual errors (namely differences between estimated values and the observed ones) of all of the stations in the model establishment subset were figured out, and they were interpolated into the whole research area in three different ways (IDW, LPI, and OK) to work out the annual and quarterly precipitation estimation residual distribution of the northeast slope of the Qinghai–Tibet Plateau. Then, five kinds of statistical indicators (Table 5) were derived from the observed values of all of the stations in a model verification subset for a quantitative analysis and inspection of the estimating effect of four methods (MSLR only, MSLR + IDW, MSLR + LPI and MSLR + OK).

In accordance with the estimating effect of models built on the basis of all of the stations (Table 7 (a)), the correlation between their estimated values and observed values almost all reached above 0.9 (except for the MSLR and MSLR + IDW estimation of winter precipitation, and the MSLR + IDW and MSLR + LPI estimation of annual precipitation). The autumn precipitation estimation model estimated best—the correlation coefficient was greater than 0.97—followed by the summer and spring estimation models, with the winter estimating model performing the worst.

Judged from the *ME*, except for the slight underestimation of precipitation in spring (−0.03–0.30%), other methods appeared to overestimate the precipitation slightly (*ME* > 0), with annual precipitation being severely overestimated (0.36–1.13%). As revealed in the *MAE* and *RMSE* analysis, the models have lower errors in estimating precipitation in spring and autumn (*MAE*: 6.81–9.44%; *RMSE*: 8.28–11.15%); the highest errors occur in winter estimations (*MAE*: 11.04–23.90%; *RMSE*: 13.76–25.09%). In spite of the vast differences in estimating the annual and seasonal precipitation, the models perform similarly in estimating precipitation within a given period of time. On the other hand, it is noteworthy that the estimation method combining multivariate linear regression with residual error distribution appeared to do better, with a higher Pearson coefficient of correlation and a lower estimation error

than the multivariate linear regression method when it was used alone. The combined method was especially good at the winter and annual precipitation estimations (with MAE falling from 23.90% to 10.64% for winter and from 12.15% to 7.73% for annual estimations, and RMSE falling from 25.09% to 13.76% for winter and from 14.08% to 9.61% for annual estimations). Generally speaking, the models that performed well in the annual and seasonal precipitation estimations were MSLR + OK (annual), MSLR + OK (spring), MSLR + IDW (summer), MSLR + OK (autumn), and MSLR + LPI (winter).

In the meantime, the performance of precipitation estimating models established (MSLRe) by station height (with 1700 m as the critical threshold) was also assessed in Table 7 (b). As revealed in the Table 7 (b), except for the summer precipitation estimation, the correlation coefficients for the other seasons and annual precipitation estimations were improved. In particular, the correlation coefficient for the spring and annual precipitation estimates was significantly improved, while the remaining models were basically the same as EM. It was higher than 0.9 for the autumn precipitation estimation, and rose from 0.90 to 0.98 for the annual precipitation estimation. As for the ME, the estimation models created based on height could effectively reduce the error so that the estimated values could be closer to the observed ones. Such a change in trend was even more evident in the annual precipitation estimation, whose minimum mean errors fell by 0.34%. The minimum mean error appeared in the MSLRe model for winter precipitation, which was only −0.01%. When it came to MAE and RMSE, the spring and annual precipitation estimating ability was also significantly improved, but the precipitation estimations of summer and autumn both slightly decreased. From an overall perspective, the annual and seasonal precipitation estimation models that were established based on height with good performance included MSLRe + LPI (annual), MSLRe + OK (spring), MSLRe (summer), MSLRe + IDW (autumn), and MSLRe + IDW (winter). Except for the spring estimation model, the other models were significantly different from the precipitation estimation models established by all of the stations.

Table 7. Statistical comparison of the estimating effect of four methods (a) for estimating models (EM), (b) for estimating models with elevation below 1700 m EMB and estimating models with elevation above 1700 m (EMA).

(a)					(b)				
Methods	R	ME/%	MAE/%	RMSE/%	Methods	R	ME/%	MAE/%	RMSE/%
Spring					Spring				
MSLR	0.93	−0.30	8.79	10.36	MSLR	0.97	−0.13	7.08	8.72
MSLR + IDW	0.92	−0.30	9.44	10.92	MSLR + IDW	0.87	0.40	11.67	17.19
MSLR + LPI	0.91	−0.30	8.59	11.15	MSLR + LPI	0.92	0.58	10.34	13.35
MSLR + OK	0.93	−0.03	8.29	10.23	MSLR + OK	0.98	0.15	5.70	6.66
Summer					Summer				
MSLR	0.91	0.86	12.69	15.29	MSLR	0.89	−0.04	8.57	11.71
MSLR + IDW	0.96	−0.08	8.10	9.24	MSLR + IDW	0.77	0.17	12.04	14.30
MSLR + LPI	0.93	0.02	9.60	10.88	MSLR + LPI	0.80	0.81	11.88	17.78
MSLR + OK	0.94	0.02	8.67	9.73	MSLR + OK	0.82	0.58	11.64	14.90
Autumn					Autumn				
MSLR	0.97	0.05	9.32	10.86	MSLR	0.94	−0.16	9.65	12.62
MSLR + IDW	0.99	0.08	8.62	10.01	MSLR + IDW	0.97	0.06	5.17	6.91
MSLR + LPI	0.99	−0.28	7.21	8.77	MSLR + LPI	0.97	0.14	6.18	9.55
MSLR + OK	0.99	−0.12	6.81	8.28	MSLR + OK	0.92	0.28	10.29	13.48
Winter					Winter				
MSLR	0.84	−1.94	23.90	25.09	MSLR	0.84	−0.01	17.36	22.50
MSLR + IDW	0.84	0.32	14.75	18.97	MSLR + IDW	0.87	0.32	12.67	16.15
MSLR + LPI	0.89	0.06	10.64	13.76	MSLR + LPI	0.86	0.48	16.40	21.03
MSLR + OK	0.86	0.10	11.04	15.34	MSLR + OK	0.86	0.07	18.13	22.42
Annual					Annual				
MSLR	0.90	0.36	12.15	14.08	MSLR	0.97	−0.18	6.64	8.24
MSLR + IDW	0.88	0.91	14.32	19.77	MSLR + IDW	0.89	0.04	10.29	12.23
MSLR + LPI	0.89	1.13	12.79	18.90	MSLR + LPI	0.98	0.02	5.88	7.19
MSLR + OK	0.97	0.54	7.73	9.61	MSLR + OK	0.86	0.05	11.71	15.63

ME: mean error, MAE: mean absolute error, RMSE: root mean square error. The bold font indicates the best among the statistic.

In accordance with the scatter distribution of the estimated annual and quarterly mean precipitation values from different models and the observed values on the northeast slope of the Qinghai–Tibet Plateau (Figure 3), it can be seen that for the estimation models established based on either all stations or height, the multivariate regression model combined with residual error distribution displayed better estimation performance than the single multivariate regression model. Such a phenomenon was more prominent in the summer and winter precipitation estimations. From the perspective of the estimation of precipitation in different periods, the annual and autumn precipitation estimations were best; the estimated values were almost equal to the observed ones. The winter precipitation estimation performance was a bit inferior. An analysis of the effectiveness of estimation models by height revealed that the estimation models built with all of the stations behaved better in the annual and autumn precipitation estimation. However, such an advantage is not significant in estimating spring precipitation. By comparison, the estimation models created by height had markedly improved performance in summer and autumn precipitation estimation, which meant that it was more proper for the precipitation estimation in the rainy season. This may be related to the influencing factors for the precipitation at different elevations on the northeast slope of the Qinghai–Tibet Plateau.

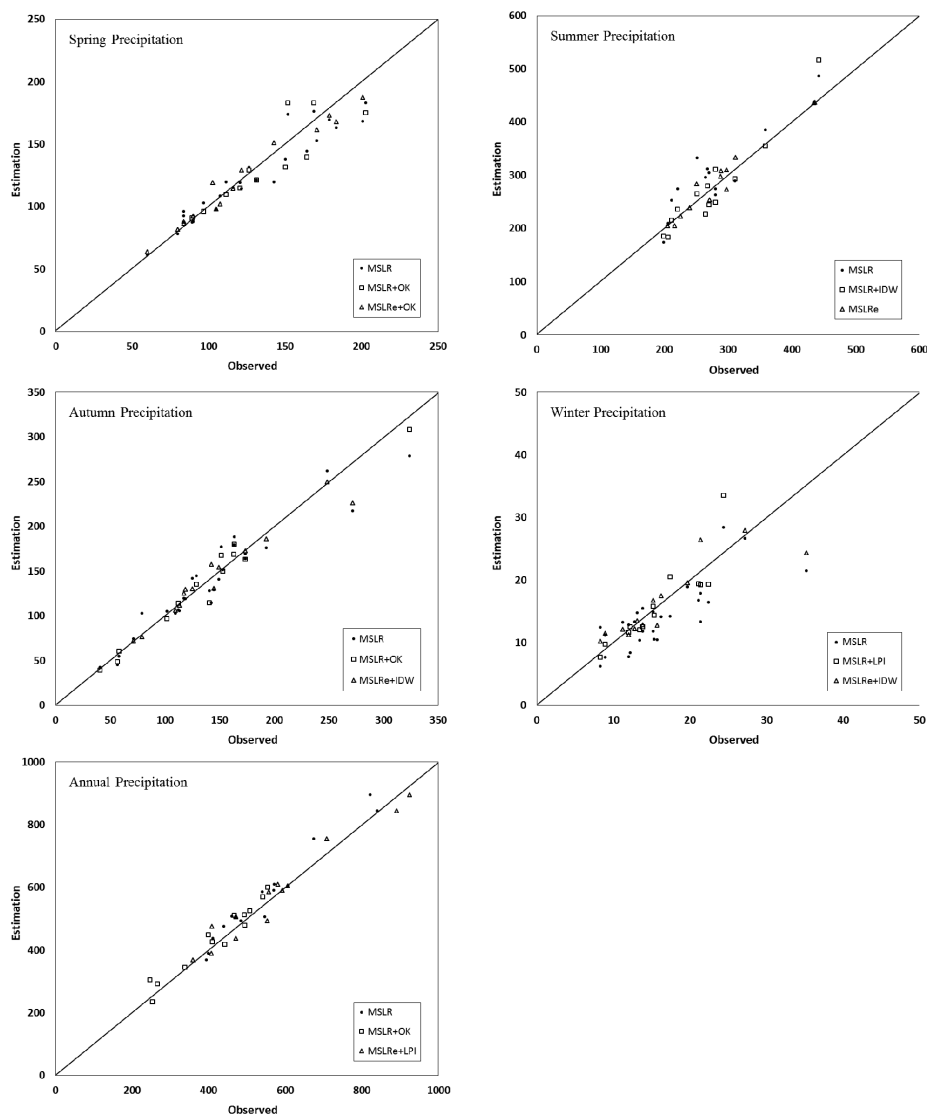


Figure 3. Scatter distribution of estimated and observed annual and quarterly precipitation values. The precipitation estimating models here include multivariable stepwise linear regression (MSLR), MSLR + inverse distance weighted (IDW)/local polynomial interpolation (LPI)/ordinary Kriging (OK) or the established multivariable stepwise linear regression (MSLRe) + IDW/LPI/OK.

5. Discussion

The northeast slope of the Qinghai–Tibet Plateau, located at the transition belt between the moist monsoon climate and the inland arid climate, is under the effect of westerlies, plateau monsoons, and complicated topographical conditions [42]. So, the precipitation distribution is diversified in this area. Disastrous weather events such as drought and violent flood occur frequently. In addition, the observation sites are sparse, which poses certain difficulties for the effective observation of precipitation events [43]. Practical observation data has been commonly used to estimate the precipitation in the unknown areas, and the observed precipitation of the known sites was always used to obtain the precipitation around the known sites by some algorithms. However, due to the complicated temporal and spatial variations in the microphysical processes of precipitation, the distribution of precipitation in different areas varies greatly. Especially in complex terrain areas (such as the typical Tibetan Plateau and slope areas), the estimation of precipitation is facing enormous challenges due to the unsatisfactory long-term remote measurement of precipitation, sparse observation sites, and poor altitude representation [44–47].

Through analyzing the correlation between many related factors and precipitation distribution, the study found that the geography and topography are the main factors that affect the annual and seasonal precipitation distributions over the northeastern slope of the Tibetan Plateau. These factors are very important for improving the precipitation estimation, especially for improving the schemes related to cloud and precipitation in numerical models [48,49]. Meanwhile, compared to the existing research results in this area [18], the multiple stepwise linear regression precipitation estimation method was established based on different geographic and topographic factors, especially the multisource regression model and residual error correction method. This method has significantly improved the ability to estimate the annual and seasonal precipitation (with the minimum *ME* is -0.01 – 0.13%), which is commendable in such complex terrain. Note that cross-validation is indeed more effective than the fixed-site verification method in selecting the optimal precipitation estimation model. This study also compared the estimation abilities of the two methods, and found that the optimal estimation model selected by cross-validation method can reduce the *RMSE* from 9.6 – 14.5% to 6.66 – 13.76% . This indicates that cross-validation can obtain effective information from limited data as much as possible, and can also reduce the over-fitting of the estimation model.

However, it should be emphasized that although the rainfall observation stations have increased in recent years, the station network density is still small (the current observation density in the study area is about 0.5 – 4 stations per 100 km^2). The resolution of data that has been used to estimate precipitation is obviously low. Thus, high-frequency observation, high-resolution observation, satellite data, and radar observation have been used by many experts and scholars to estimate precipitation due to their wide observation range [50–52]. Future work will follow up on the idea of combining satellite and radar observations to develop a higher resolution and more accurate precipitation estimation for areas with complex terrain.

6. Conclusions

The study first studied the relationship between the seasonal and annual mean precipitation distribution and the 11 geographical or topographical factors on the northeast slope of the Qinghai–Tibet Plateau, and created multivariate linear regression precipitation estimating models based on the studied relationship. Then, a residual error correction method was employed to improve the overall performance of the estimation models. Finally, the suitability of the different estimation methods for the area were analyzed.

The research indicates that the precipitation on the northeast slope of the Qinghai–Tibet Plateau is differentiated at the elevation of 1700 m . That is, precipitation distributions obtained by the stations below 1700 m and above 1700 m presented distinct features. For the stations below 1700 m , significant and extremely negative correlation is spotted between the annual and quarterly mean precipitation and elevation and latitude, respectively. In contrast, the annual and quarterly mean

precipitation is significantly and positively related to the longitude as well as the average slope of the station's vicinity. Steeper terrain is inclined to have higher precipitation. In spring, summer, and autumn, the precipitation is remarkably and positively related to the maximum elevation in the west, where the major regional water vapor comes from. For the stations above 1700 m, the annual and quarterly mean precipitation is significantly and negatively associated with the latitude, and so is the precipitation in spring, summer, and winter. On the other hand, the annual and quarterly mean precipitation is obviously and positively related to the elevation, which constitutes the major difference between the stations above 1700 m and below 1700 m. Both annual mean precipitation and the mean precipitation in spring, summer, and winter are positively related to the exposure, which means that the more westward and northward the station's vicinity, the higher the precipitation. In the meantime, the annual, spring, summer, and autumn mean precipitation are positively related to the highest elevation in four directions.

Annual and quarterly mean precipitation estimating models were established by all of the stations and height on the basis of geographical and topographical factors through a multivariate stepwise linear regression method. An analysis of the adjusted \bar{R}^2 values of the models proves that the autumn, summer, spring, and annual mean precipitation estimation is better, while the winter precipitation estimation is less satisfactory. Residual error interpolation correction can effectively improve the estimation performance of the multivariate regression model, since the models that did well in the annual and seasonal precipitation estimation all combined the multivariate regression with residual error correction. However, different residual error interpolations were adopted for different seasons. The multivariate regression model combined with residual error correction established by elevation seems to be better at estimating the precipitation in the rainy season.

The research in this paper demonstrates that the method of multivariate regression combined with residual calibration can effectively improve the estimation ability of rainy season precipitation, which provides a new idea for precipitation estimation in the complex terrain of the northeast slope of the Qinghai–Tibet Plateau. In addition, the altitude of 1700 m as the threshold of precipitation distribution in the region provides new clues that can enhance the understanding of precipitation distribution in the region. Research can also provide recommendations for future actions to improve understandings of management and the prediction of droughts and floods in the region.

Author Contributions: This research work was mainly conducted by W.L. at Lanzhou University of China. He also compiled the manuscript. Q.Z. is the principle investigator on the project. Z.F., H.L. and X.C. contributed with results analysis and revision of the manuscript.

Funding: The authors gratefully acknowledge the financial support provided by the National Natural Science Foundation of China (No. 41505036, 41630426) and Gansu Meteorological Technical Innovation Team Project (No. GSQXCXTD-2017-01).

Conflicts of Interest: The authors declare no conflict of interest.

References

1. Sangati, M.; Borga, M. Influence of rainfall spatial resolution on flash flood modelling. *Nat. Hazards Earth Syst. Sci.* **2009**, *9*, 575–584. [[CrossRef](#)]
2. Rana, A.; Uvo, C.B.; Bengtsson, L.; Sarthi, P. Trend analysis for rainfall in Delhi and Mumbai, India. *Clim. Dyn.* **2012**, *38*, 45–56. [[CrossRef](#)]
3. Gao, T.; Xie, L. Study on progress of the trends and physical causes of extreme precipitation in China during the last 50 years. *Adv. Earth Sci.* **2014**, *29*, 577–589. (In Chinese) [[CrossRef](#)]
4. Wu, G.; Wang, J.; Liu, X.; Liu, Y. Numerical modeling of the influence of Eurasian orography on the atmospheric circulation in different seasons. *Acta Meteorol. Sin.* **2005**, *63*, 603–612. (In Chinese)
5. Beniston, M. Mountain weather and climate: A general overview and a focus on climatic change in the Alps. *Hydrobiologia* **2006**, *562*, 3–16. [[CrossRef](#)]
6. Zhu, S.; Xu, D.; Xu, M. Structure and Distribution of Rainfall over Mesoscale Mountains in the Asian Summer Monsoon Region. *Chin. J. Atmos. Sci.* **2010**, *34*, 71–82. (In Chinese)

7. Qi, Y.; Fang, S.; Zhou, W. Correlative analysis between the changes of surface solar radiation and its relationship with air pollution, as well as meteorological factor in East and West China in recent 50 years. *Acta Phys. Sin.* **2015**, *64*, 089201. (In Chinese) [[CrossRef](#)]
8. Morin, E.; Gabella, M. Radar-based quantitative precipitation estimation over Mediterranean and dry climate regimes. *J. Geophys. Res.* **2007**, *112*, 365–371. [[CrossRef](#)]
9. Al-Ahmadi, K.; Al-Ahmadi, S. Spatiotemporal variations in rainfall-topographic relationships in southwestern Saudi Arabia. *Arab. J. Geosci.* **2014**, *7*, 3309–3324. [[CrossRef](#)]
10. Saeidabadi, R.; Najafi, M.; Roshan, G.; Fitchett, J.; Abkharabat, S. Modelling spatial, altitudinal and temporal variability of annual precipitation in mountainous regions: The case of the Middle Zagros, Iran. *Asia Pac. J. Atmos. Sci.* **2016**, *52*, 437–449. [[CrossRef](#)]
11. Portalés, C.; Boronat, N.; Pardo-Pascual, J.; Balaguer-Beser, A. Seasonal precipitation interpolation at the Valencia region with multivariate methods using geographic and topographic information. *Int. J. Clim.* **2010**, *30*, 1547–1563. [[CrossRef](#)]
12. Marquinez, J.; Lastra, J.; Garcia, P. Estimation models for precipitation in mountainous regions: The use of GIS and multivariate analysis. *J. Hydrol.* **2003**, *270*, 1–11. [[CrossRef](#)]
13. Shu, S.; Wang, Y.; Xiong, A. Estimation and analysis for geographic and orographic influences on precipitation distribution in China. *Chin. J. Geophys.* **2007**, *50*, 1703–1712. (In Chinese) [[CrossRef](#)]
14. Shu, S.; Yu, Z.; Wang, Y.; Bai, M. A statistic model for the spatial distribution of precipitation estimation over the Tibetan complex terrain. *Chin. J. Geophys.* **2005**, *48*, 535–542. (In Chinese) [[CrossRef](#)]
15. Zhao, C.; Feng, Z.; Nan, Z. Modelling the Temporal and Spatial Variabilities of Precipitation in Zulihe River Basin of the Western Loess Plateau. *Plateau Meteorol.* **2008**, *27*, 208–214. (In Chinese)
16. Du, L.; Li, J.; Chen, X.; Shang, K.; Yang, D.; Wang, S. Analysis on Cloud and Vapor Flux in the Northeast of the Qinghai-Tibet Plateau during the Period from 2001 to 2011. *Arid Zone Res.* **2012**, *29*, 862–869. (In Chinese)
17. Zhang, J.; Li, D.; He, J.; Wang, X. Influence of terrain on precipitation distribution in Qingzang tableland in wet and dry years. *Adv. Water Sci.* **2007**, *18*, 319–326.
18. Wei, H.; Li, J.; Liang, T. Study on the estimation of precipitation resources for rainwater harvesting agriculture in semi-arid land of China. *Agric. Water Manag.* **2005**, *71*, 33–45. [[CrossRef](#)]
19. Peng, S.; Zhao, C.; Wang, X.; Xu, Z.; Liu, X.; Hao, H.; Yang, S. Mapping Daily Temperature and Precipitation in the Qilian Mountains of Northwest China. *J. Mt. Sci.* **2014**, *11*, 896–905. [[CrossRef](#)]
20. Yu, Y.; Wei, W.; Chen, L.; Yang, L.; Zhang, H. Comparison on the methods for spatial interpolation of the annual average precipitation in the Loess Plateau region. *Chin. J. Appl. Ecol.* **2015**, *26*, 999–1006. (In Chinese)
21. National Meteorological Information Center. Standard Monthly Dataset of Chinese Surface Climate. Available online: <http://data.cma.cn> (accessed on 5 August 2017).
22. Ren, Z.; Xiong, A.; Zou, F. The Quality Control of Surface Monthly Climate Data in China. *J. Appl. Meteorol. Sci.* **2007**, *18*, 516–523. (In Chinese)
23. Liu, W.; Zhang, Q.; Fu, Z. Variation Characteristics of Precipitation and Its Affecting Factors in Northwest China over the Past 55 Years. *Plateau Meteorol.* **2017**, *36*, 1533–1545. (In Chinese) [[CrossRef](#)]
24. National Aeronautics and Space Administration (NASA) and National Geospatial-Intelligence Agency (NGA). SRTM Data Set. Available online: <http://srtm.csi.cgiar.org/index.asp> (accessed on 14 October 2017).
25. Donges, J.F.; Petrova, I.; Loew, A.; Marwan, N.; Kurths, J. How complex climate networks complement eigen techniques for the statistical analysis of climatological data. *Clim. Dyn.* **2013**, *45*, 2407–2424. [[CrossRef](#)]
26. Diaconescu, E.P.; Gachon, P.; Scinocca, P.; Laprise, R. Evaluation of daily precipitation statistics and monsoon onset/retreat over western Sahel in multiple data sets. *Clim. Dyn.* **2014**, *45*, 1325–1354. [[CrossRef](#)]
27. Draper, N.R.; Smith, H. *Applied Regression Analysis*, 3rd ed.; Wiley: New York, NY, USA, 1998.
28. Kohavi, R. A study of cross-validation and bootstrap for accuracy estimation and model selection. In Proceedings of the Fourteenth International Joint Conference on Artificial Intelligence, Montreal, QC, Canada, 20–25 August 1995; Morgan Kaufmann: San Mateo, CA, USA, 1995; pp. 1137–1143.
29. Hastie, T.; Tibshirani, R.; Friedman, J.H. *The Elements of Statistical Learning: Data Mining Inference and Prediction*; Springer: New York, NY, USA, 2001.
30. Bartier, P.M.; Keller, C.P. Multivariate interpolation to incorporate thematic surface data using inverse distance weighting. *Comput. Geosci.* **1996**, *22*, 795–799. [[CrossRef](#)]
31. Daly, C. Guidelines for assessing the suitability of spatial climate data sets. *Int. J. Clim.* **2006**, *26*, 707–721. [[CrossRef](#)]

32. Fatichi, S.; Caporali, E. A comprehensive analysis of changes in precipitation regime in Tuscany. *Int. J. Clim.* **2009**, *29*, 1883–1893. [[CrossRef](#)]
33. Francisco, M.; Vilar, J.M. Local polynomial regression estimation with correlated errors. *Commun. Stat.* **2001**, *30*, 1271–1293. [[CrossRef](#)]
34. Williams, C.K.I. *Prediction with Gaussian Processes: From Linear Regression to Linear Prediction and Beyond*; Springer: Dordrecht, The Netherlands, 1989.
35. Morlier, J.; Chermain, B.; Gourinat, Y. Original statistical approach for the reliability in modal parameters estimation. *J. Hazard. Mater.* **2009**, *114*, 240–248.
36. Hyndman, R.J.; Koehler, A.B. Another look at measures of forecast accuracy. *Int. J. Forecast.* **2006**, *22*, 679–688. [[CrossRef](#)]
37. Harris, G.N.; Bowman, K.P.; Shin, D.B. Comparison of freezing-level altitudes from the NCEP reanalysis with TRMM precipitation radar brightband data. *J. Clim.* **2000**, *13*, 4137–4148. [[CrossRef](#)]
38. Zhao, A.; Zhang, M.; Sun, M.; Wang, B.; Wang, S.; Wang, Q. Changes in 0 °C isotherm height of Southwest China during 1960–2010. *Acta Geogr. Sin.* **2013**, *68*, 994–1006. (In Chinese)
39. Chen, Z.; Chen, Y.; Li, W. Response of runoff to change of atmospheric 0 °C level height in summer in arid region of Northwest China. *Sci. China Earth Sci.* **2012**, *55*, 1533–1544. [[CrossRef](#)]
40. Chen, T.Y.; Li, Z.R.; Chen, Q.; Li, B.Z. The Analysis of Climate Characteristics of Water Vapor Distribution over Northwest China with Water Vapor Field Retrieved from GMS5 Satellite Data. *Chin. J. Atmos. Sci.* **2005**, *29*, 864–871.
41. Wang, X.; Xu, X.; Wang, W. Characteristic of Spatial Transportation of Water Vapor for Northwest China's Rainfall in Spring and Summer. *Plateau Meteorol.* **2007**, *26*, 749–758. (In Chinese)
42. Zhang, Z.; Zhang, Q.; Zhao, Q.; Zhang, L.; Cai, Y. Radar quantitative precipitation inversion and its application to areal rainfall estimation in the northeastern marginal areas of the Tibetan Plateau. *J. Glaciol. Geocryol.* **2013**, *35*, 621–629. (In Chinese) [[CrossRef](#)]
43. Xu, X.; Du, Y.G.; Tang, J.P.; Wang, Y. Variations of temperature and precipitation extremes in recent two decades over China. *Atmos. Res.* **2011**, *101*, 143–154. [[CrossRef](#)]
44. Mizukami, N.; Smith, M.B. Analysis of inconsistencies in multi-year gridded quantitative precipitation estimate over complex terrain and its impact on hydrologic modeling. *J. Hydrol.* **2012**, *428–429*, 129–141. [[CrossRef](#)]
45. Delbari, M.; Afrasiab, P.; Jahani, S. Spatial interpolation of monthly and annual rainfall in northeast of Iran. *Meteorol. Atmos. Phys.* **2013**, *122*, 103–113. [[CrossRef](#)]
46. Gou, Y.; Ma, Y.; Chen, H.; Wen, Y. Radar-derived quantitative precipitation estimation in complex terrain over the eastern Tibetan Plateau. *Atmos. Res.* **2018**, *203*, 286–297. [[CrossRef](#)]
47. Henn, B.; Newman, A.J.; Livneh, B.; Daly, C.; Lundquist, J.D. An assessment of differences in gridded precipitation datasets in complex terrain. *J. Hydrol.* **2018**, *556*, 1205–1209. [[CrossRef](#)]
48. Colle, B.A.; Mass, C.F.; Westrick, K.J. Mesoscale modeling of precipitation in complex orography along the west coast of North America. In Proceedings of the 8th Conference on Mountain Meteorology, Flagstaff, AZ, USA, 3–7 August 1998.
49. Junquas, C.; Li, L.; Vera, C.S.; Treut, H.L.; Takahashi, K. Influence of South America orography on summertime precipitation in Southeastern South America. *Clim. Dyn.* **2016**, *46*, 3941–3963. [[CrossRef](#)]
50. Fortin, V.; Roy, G.; Donaldson, N.; Mahidjiba, A. Assimilation of radar quantitative precipitation estimations in the Canadian Precipitation Analysis (CaPA). *J. Hydrol.* **2015**, *531*, 296–307. [[CrossRef](#)]
51. Rafieeinassab, A.; Norouzi, A.; Seo, D.-J.; Nelson, B. Improving high-resolution quantitative precipitation estimation via fusion of multiple radar-based precipitation products. *J. Hydrol.* **2015**, *531*, 320–336. [[CrossRef](#)]
52. Zhao, H.; Yang, B.; Yang, S.; Huang, Y.; Dong, G.; Bai, J.; Wang, Z. Systematical estimation of GPM-based global satellite mapping of precipitation products over China. *Atmos. Res.* **2018**, *201*, 206–217. [[CrossRef](#)]

